Molecular Systems Biology 6; Article number 402; doi:10.1038/msb.2010.58
Citation: ***Molecular Systems Biology*** **6:402**

www.molecularsystemsbiology.com

molecular systems biology

microRNA-122 as a regulator of mitochondrial metabolic gene network in hepatocellular carcinoma

Julja Burchard[1,8,12], Chunsheng Zhang[1,9,12], Angela M Liu[2,3,12], Ronnie TP Poon[2], Nikki PY Lee[2], Kwong-Fai Wong[2,4], Pak C Sham[5], Brian Y Lam[6], Mark D Ferguson[1,9], George Tokiwa[1,10], Ryan Smith[1,9], Brendan Leeson[1], Rebecca Beard[1], John R Lamb[1,11], Lee Lim[1,8], Mao Mao[1,11], Hongyue Dai[1,9] and John M Luk[2,3,4,7,*]

[1] Rosetta Inpharmatics LLC, a wholly-owned subsidiary of Merck and Co., Inc., Seattle, WA, USA, [2] Department of Surgery, The University of Hong Kong, Queen Mary Hospital, Hong Kong, Hong Kong, [3] Department of Pharmacology, National University of Singapore, Singapore, Singapore, [4] Cancer Science Institute, National University of Singapore, Singapore, Singapore, [5] Department of Psychiatry, The University of Hong Kong, Hong Kong, Hong Kong, [6] Metabolic Research Laboratories, Institute of Metabolic Science, University of Cambridge, Addenbrooke's Hospital, Cambridge, UK and [7] Department of Surgery, National University of Singapore, Singapore, Singapore
[8] Present address: Sirna Therapeutics, a wholly-owned subsidiary of Merck and Co., Inc., San Francisco, CA 94158, USA
[9] Present address: Merck Research Laboratories, 33 Avenue Louis Pasteur, Boston, MA 02115, USA
[10] Present address: Merck & Co., Inc, Upper Gwynned, PA 19454, USA
[11] Present address: Pfizer Inc., 10724 Science Center Drive, San Diego, CA 92121, USA
[12] These authors contributed equally to this work
* Corresponding author: Department of Pharmacology, NUHS, National University of Singapore, 10 Medical Drive, MD11 #05-09, Singapore 117597, Singapore. Tel.: +65 65 16 4516; Fax: +65 68 73 7690; E-mail: jmluk@nus.edu.sg

Received 5.11.09; accepted 29.6.10

Tumorigenesis involves multistep genetic alterations. To elucidate the microRNA (miRNA)–gene interaction network in carcinogenesis, we examined their genome-wide expression profiles in 96 pairs of tumor/non-tumor tissues from hepatocellular carcinoma (HCC). Comprehensive analysis of the coordinate expression of miRNAs and mRNAs reveals that miR-122 is under-expressed in HCC and that increased expression of miR-122 seed-matched genes leads to a loss of mitochondrial metabolic function. Furthermore, the miR-122 secondary targets, which decrease in expression, are good prognostic markers for HCC. Transcriptome profiling data from additional 180 HCC and 40 liver cirrhotic patients in the same cohort were used to confirm the anti-correlation of miR-122 primary and secondary target gene sets. The HCC findings can be recapitulated in mouse liver by silencing miR-122 with antagomir treatment followed by gene-expression microarray analysis. *In vitro* miR-122 data further provided a direct link between induction of miR-122-controlled genes and impairment of mitochondrial metabolism. In conclusion, miR-122 regulates mitochondrial metabolism and its loss may be detrimental to sustaining critical liver function and contribute to morbidity and mortality of liver cancer patients.
Molecular Systems Biology **6**: 402; published online 24 August 2010; doi:10.1038/msb.2010.58
Subject Categories: functional genomics; molecular biology of disease
Keywords: hepatocellular carcinoma; microarray; miR-122; mitochondrial; survival

Introduction

Hepatocellular carcinoma (HCC) is one of the most aggressive human malignancies, common in Asia, Africa, and the areas with endemic infections of hepatitis-B or -C viruses (HBV or HCV) (But *et al*, 2008). It has the third highest mortality rate among cancers worldwide and since the 1990s, the second highest cancer mortality rate in China. Globally, the 5-year survival rate of HCC is $<5\%$ and $\sim 600\,000$ HCC patients die each year (Parkin *et al*, 2005; Hao *et al*, 2009). The high mortality associated with this disease is mainly attributed to the failure to diagnose HCC patients at an early stage and a lack of effective therapies for patients with advanced stage HCC. Although surgery remains the most effective treatment for HCC, the majority of patients are inoperable at presentation because of late diagnosis (Lee *et al*, 2007; Sun *et al*, 2007). The consequent improvement in long-term survival of post-surgery patients is only modest because of a high recurrence rate of intrahepatic metastases that develop through invasion of the portal vein or spread to other parts of the liver (Poon *et al*, 2001). Understanding the relationships between phenotypic and molecular changes in HCC is of paramount

importance to develop new diagnosis and treatment of HCC and improve the prognosis of diagnosed patients.

Although expression of many mRNAs and microRNAs (miRNAs) has been shown to differ between tumor and non-tumor tissue (Croce, 2008), the direct relevance of such differential regulation is unclear. Changes in chromosomal DNA, in expression of miRNAs, or other transcriptional/post-transcriptional regulators may contribute to the coordinate regulation of groups of transcripts, driving tumor progression. Expression of additional miRNAs and mRNAs may subsequently change in further driving the process of carcinogenesis or in responding to it. Driver miRNAs may be distinguished from responder miRNAs by characteristics of miRNA targeting (Lim *et al*, 2005) in coordinately regulated mRNAs (Linsley *et al*, 2007). In the simplest case, miRNAs driving differential expression should be anti-correlated with their targets, that is over-expressed in tissues with decreased target transcript expression and under-expressed in tissues with increased target transcript expression.

We examined mRNA- and miRNA-expression profiles of tumor and adjacent non-tumor liver tissue from HCC patients. The patient population was selected from a region of endemic HBV infection, and HBV infection appears to contribute to the etiology of HCC in these patients. About 88% of the patients in this study tested positive for HBV antigen; patients testing positive for HCV antigen were excluded. In these HCC patients, who were found to be generally under-expressing miR-122 relative to the control population and in mice treated with miR-122 antagomir, miR-122 expression was both inversely correlated with expression of genes bearing potential target sites for miR-122 and positively correlated with expression of pathways related to liver metabolic function. These results suggest that miR-122 regulation of transcripts may be a driver of differences in metabolic function between tumor and adjacent non-tumor tissue, and within each tissue type and extend literature reports of the association of miR-122-expression levels with lipid metabolism (Jopling *et al*, 2005; Esau *et al*, 2006; Elmén *et al*, 2008a, b; Coulouarn *et al*, 2009) and suppressing the metastatic properties of HCC (Tsai *et al*, 2008; Coulouarn *et al*, 2009).

Results

Integrating miRNA- and mRNA-expression profiling

We conducted mRNA- and miRNA-expression profiling on tumor and adjacent non-tumor tissues from 96 HCC patients. Among 220 miRNAs profiled, miR-122 is the most highly expressed miRNA in tumor and in adjacent non-tumor liver tissue (Figure 1A), agreeing well with published work (Lagos-Quintana *et al*, 2002). On average, adjacent non-tumor liver tissue contained ~150 000 copies of miR-122 per 10 pg (approximately one cell) of input RNA. In addition, miR-122 expression was decreased in tumor tissue relative to non-tumor tissue with an average level almost two-fold lower than in adjacent liver tissue (Figure 1B), ranking 14th out of 220 miRNAs for decreased expression in HCC by rank-sum *P*-value, and showing the largest absolute change in expression between HCC and adjacent non-tumor tissue, confirming earlier observations (Kutay *et al*, 2006; Budhu *et al*, 2008). miR-122 was expressed more variably in tumors than in corresponding non-tumor tissues (the s.d. of log10 expression level is 0.30 in tumor versus 0.13 in non-tumor). miRNAs whose expression was reduced comparably or even more significantly than miR-122 in HCC include miR-139, miR-99a, miR-10a, miR-199a/miR-199a*, miR-450, miR-378, miR-125b, miR-214, miR-422b, miR-424, miR-451, and miR-101. In 34 patients suffering from cirrhosis without HCC, miR-122 was reduced approximately three-fold relative to levels in non-tumor tissue from HCC patients, and across in all tissues examined miR-122 was reduced ~25% in the presence versus in the absence of hepatitis-B antigen expression (data not shown), suggesting that liver diseases other than HCC may also decrease miR-122 expression.

To identify transcripts whose expression was associated with expression of particular miRNAs, we scored transcripts for correlation of their expression levels with the expression levels of 220 human miRNAs in the 96 paired tumor and adjacent non-tumor tissues. Transcripts correlated with miRNAs with correlation coefficients >0.5 or <−0.5 were identified. Over

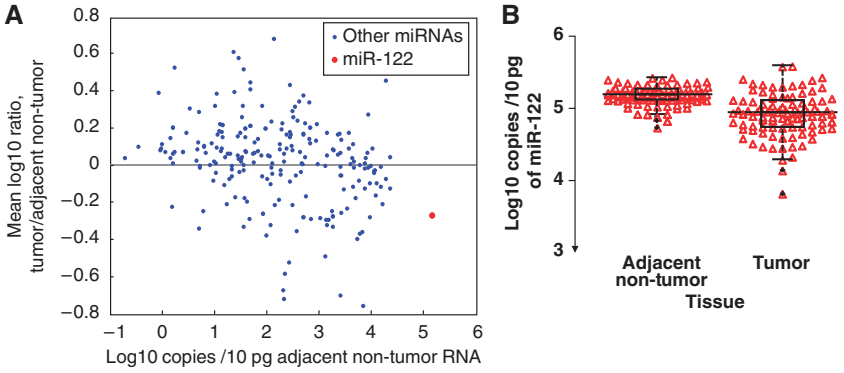

Figure 1 miR-122 is the most abundant miRNA in adjacent non-tumor liver tissue, and its expression is reduced on average and more variable in HCC tumors. (**A**) Expression levels of 220 human miRNAs in tumor and adjacent non-tumor tissue; *x* axis: average expression levels in copies per 10 pg of mRNA; *y* axis: average of the log10 ratios of miRNA expression in each tumor to the mean-expression level for that miRNA in adjacent non-tumor tissue. (**B**) Expression levels of miR-122 in paired adjacent non-tumor (left) and tumor tissues from 96 HCC patients. Triangles represent individual subjects, whereas the box-plots show the median (horizontal bar), 25th–75th percentile range (box), 1.5 times the interquartile range (whiskers) and outliers (plusses) of the distribution of miR-122 expression. MiR-122 was significantly differentially expressed between tumor and adjacent non-tumor liver tissues (rank-sum *P*-value, 1.75e–13; miR-122 ranked 14th of 220 miRNAs).

1000 transcripts were correlated and over 1000 transcripts were anti-correlated with miR-122 at this level. Among the 220 miRNAs profiled, only 13 miRNAs were found correlated with $\geqslant$1000 transcripts and anti-correlated with $\geqslant$1000 transcripts.

Identification of driver miRNA

To determine which of the miRNAs might be driving expression of its correlated transcripts, we examined the sets of correlated or anti-correlated genes for miRNA seed region enrichment in their 3′UTRs (Lim *et al*, 2005). We calculated the hypergeometric *P*-value for enrichment of the seed sequences of each miRNA in the 3′UTRs of its correlated and anti-correlated genes, and found 13 miRNAs with expectation or *E*-value <0.01 (*P*-value corrected for testing of 4096 hexamers) that remained significant after further correction for examination of 241 miRNA-correlated gene sets (Figure 2). As a control, for each set of mRNAs correlated to a particular miRNA, we also examined enrichment for seed matches to all other miRNAs. Only miR-122 negatively correlated genes showed more significant enrichment for seed matches to the correlated miRNA itself than for seed matches to all other miRNAs, and retained significance after correcting for examination of 241 gene sets. The miR-122 correlated and anti-correlated genes are displayed in Supplementary Figure 1.

Characterization of miR-122-associated transcripts

Transcripts anti-correlated with miR-122 are potential miR-122 targets. The transcripts most highly anti-correlated with miR-122 expression were highly enriched for the presence of the miR-122 central seed hexamer, CACTCC, in the 3′UTR. Among the 1106 negatively correlated transcripts, 321 of 892 annotated transcripts contained the 3′UTR hexamer CACTCC, out of 4097 total transcripts containing that hexamer. This hexamer was ranked most highly by enrichment test with a hypergeometric *E*-value of enrichment of 5e−33. In general, the miR-122 negatively correlated transcripts were enriched for cell-cycle genes (among KEGG Pathways, 'cell-cycle' ranked most highly with an *E*-value of 4e−18, 35 of 199 annotated genes overlapped with 109 'cell-cycle' genes). Surprisingly, those negatively correlated CACTCC seed-matched genes were not significantly enriched for cell-cycle annotation ($E>0.01$) and did not significantly overlap with the negatively correlated cell-cycle genes. The data suggests that miR-122 is unlikely to directly regulate the cell cycle in these patients. Thus, the seed-matched genes had no significant KEGG Pathway annotation.

Transcripts positively correlated with miR-122 were not enriched for 3′UTR seed matches to miR-122. Interestingly, these 1042 transcripts were enriched for genes coding for mitochondrially localized proteins (among GO Cellular Components, 'mitochondrion' ranked most highly with an *E*-value=9e−33, 117 of 562 annotated genes overlapped with 785 'mitochondrion' genes) and for metabolic functions (among KEGG Pathways, 'fatty-acid metabolism' ranked most highly with an *E*-value=5e−16, 27 of 307 annotated genes overlapped with 49 'fatty-acid metabolism' genes; 'valine, leucine, and isoleucine degradation' ranked No. 2, *E*-value=9e−13, 23 of 307 annotated genes overlapped with

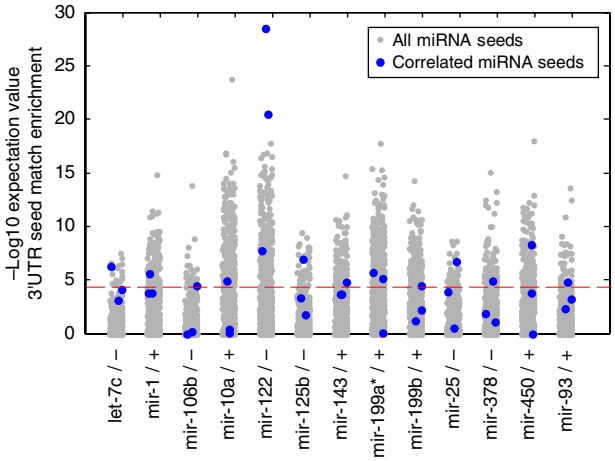

Figure 2 miR-122 is the miRNA most strongly associated with seed-matched genes in tumor and adjacent non-tissues. Transcripts whose expression levels were correlated or anti-correlated with expression levels of miRNAs were tested for enrichment of 3′UTR hexamers (seed sequences) by the hypergeometric *P*-value. Shown are the *E*-values (Bonferroni-corrected *P*-values adjusted for testing of 4096 hexamers) for enrichment of the three hexamers matching bases 1–8 of the correlated miRNA (blue dots) or bases 1–8 of other known miRNAs (gray dots). Each column shows log10 *E*-values for a set of transcripts significantly positively or negatively correlated with a particular miRNA. The direction of correlation is indicated by '+' for positive and '−' for negative or anti-correlation. Only those transcript sets are shown for which the correlated miRNA has an *E*-value of <0.01, after further adjustment for the 241 transcript sets examined, for at least one of its 3′UTR seed hexamers in a correlated or anti-correlated transcript set. The red dashed line marks $E<0.01$ after adjustment for both 4096 hexamers tested per transcript set and for the 241 transcript sets examined.

44 'valine, leucine, and isoleucine degradation' genes). The great majority of transcripts involved in fatty-acid and amino-acid metabolism were mitochondrially localized, with highly significant overlap between all three pairwise comparisons (single-test hypergeometric *P*-values—mitochondrion/fatty-acid metabolism overlap: *P*=7.4e−12; mitochondrion/valine–leucine–isoleucine degradation overlap: *P*=6.2e−22; fatty-acid metabolism/valine–leucine–isoleucine degradation overlap: *P*=3.1e−9). Thus, miR-122 expression appeared positively associated with mitochondrially related metabolic functions in human liver.

In vivo validation of the miR-122-regulated genes

We wanted to test whether the seed-matched genes were directly targeted by miR-122, and further, whether the transcripts encoding mitochondrially localized proteins were regulated as a consequence of miR-122 expression independent of tumor status. To test the direct and indirect effects of loss of miR-122 alone, *in vivo* silencing of miR-122 was performed by antisense inhibition of miR-122 (anti-miR-122) in wild-type mice. Either 1 week or 4 weeks (Esau *et al*, 2006) post-treatment, livers were subjected to microarray profiling (Figure 3A). We examined the consensus of multiple animals to minimize issues associated with animal-to-animal and array-to-array variations in gene expression. A total of 689 up-regulated transcripts from the consensus of both time points were enriched for 3′UTR matches to the central miR-122 seed hexamer CACTCC in both human and mouse miR-122 (3′UTR hexamer 'CACTCC' ranked most highly by enrichment

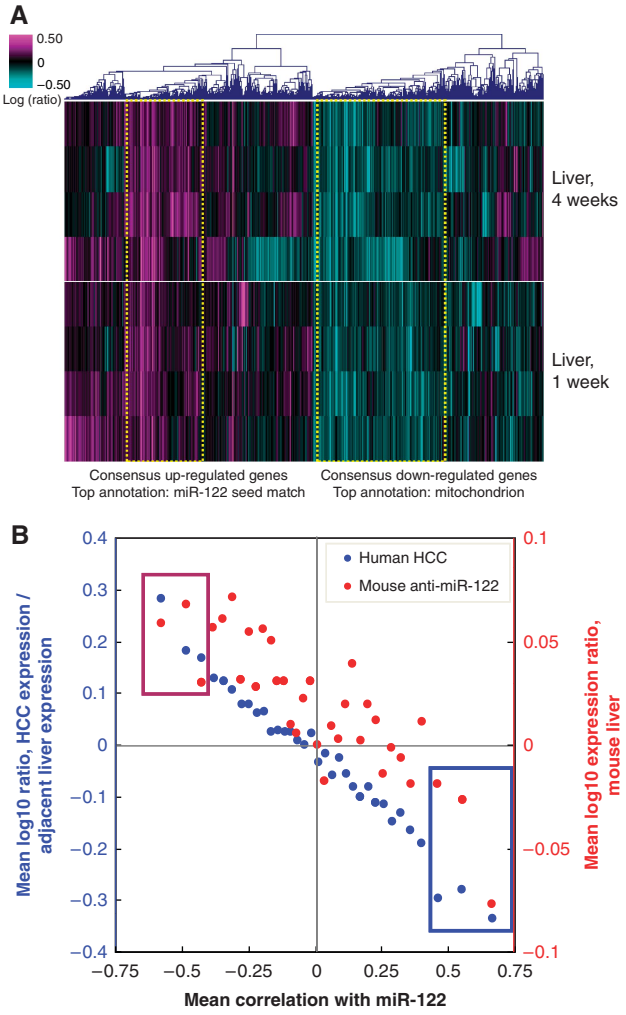

Figure 3 (**A**) Seed-matched genes are up-regulated and mitochondrial genes are down-regulated after inhibition of miR-122. Shown are the liver-expression profiles of mice treated twice weekly with anti-miR-122 for 4 weeks (top four profiles) or 1 week (bottom four profiles). Transcripts regulated in at least one experiment with *P*-value of regulation <0.05 are shown. Boxes identify consensus up-regulated and consensus down-regulated transcripts. Consensus up-regulated transcripts were enriched for 3′UTR matches to CACTCC, the central miR-122 seed hexamer. Consensus down-regulated genes were enriched for mitochondrially localized gene products. (**B**) Correlation to miR-122 in human HCC predicts ortholog regulation by anti-miR-122 in mouse livers. Shown is the relationship between transcript correlation with miR-122 levels in HCC and adjacent liver tissue and changes in expression in HCC tumor and adjacent non-tumor tissues, and in anti-miR-122-treated mice. Human/mouse ortholog pairs are binned by the correlation coefficient of the human ortholog with miR-122, at a rate of $\sim$1000 human orthologs per bin. The ortholog pairs within each bin are then restricted to those whose mouse ortholog is regulated with $P<0.05$ by anti-miR-122. For each bin, the mean correlation coefficient of the human ortholog is plotted against the mean-expression ratios in both human and mouse contexts. Left axis/blue dots: the log10 ratio of mean tumor expression to mean adjacent tissue expression is shown for the human orthologs in each bin. Right axis/red dots: the mean log10 expression ratio of regulation by anti-miR-122 is shown for the mouse orthologs in each bin. Purple box: putative primary miR-122 targets; blue box: putative secondary miR-122 targets. Source data is available for this figure at www.nature.com/msb.

test, with an *E*-value=5e−83, 350 of 639 annotated genes overlapped with 3904 CACTCC hexamer-containing genes). As with the genes negatively correlated with miR-122 in HCC patients, no significant biological annotation was associated with the seed-matched genes up-regulated by anti-miR-122 in mouse livers. The most significant biological annotation for 1865 consensus down-regulated genes was mitochondrial localization (among GO Cellular Components, 'mitochondrion' ranked most highly, *E*-value=2.5e−72, 219 of 1180 annotated genes overlapped with 663 'mitochondrion' genes). Enrichment for mitochondrially localized gene products was not observed in genes down-regulated in treatments by antagonists to other miRNAs (data not shown). The mitochondrial genes down-regulated by anti-miR-122 treatment were enriched for metabolic functions (among KEGG Pathways, 'oxidative phosphorylation' ranked most highly, *E*-value=5e−20, 53 of 540 annotated genes overlapped with 116 'oxidative phosphorylation' genes; 'valine, leucine, and isoleucine degradation' ranked No. 2, *E*-value=6e−8, 21 of 540 annotated genes overlapped with 43 genes in this set; 'fatty-acid metabolism' ranked No. 3, *E*-value=2e−5, 18 of 540 annotated genes overlapped with 43 genes in this set). These results confirm our observations in human HCC samples and show that loss of miR-122 alone can up-regulate seed-matched genes and down-regulate mitochondrially localized genes that are critical for metabolic functions.

Characterization of miR-122-regulated orthologous genes

To the extent that miR-122 targeting is conserved from mouse to human, we can expect mouse genes up-regulated by anti-miR-122 to be orthologous to human genes anti-correlated with miR-122 in HCC. Further, if biological pathways regulated by miR-122 are conserved as well, mouse orthologs of genes positively correlated with miR-122 should be down-regulated by anti-miR-122. To this end, we compared the mouse signature genes with human genes anti-correlated and correlated with miR-122. Restricting the analysis to orthologs represented on the human and the mouse microarrays among both putative direct targets and putative downstream targets, human and mouse genes showed significant overlap for regulations in the same direction (overlap of human genes anti-correlated with miR-122 and mouse genes up-regulated by anti-miR-122; hypergeometric *P*-value=2.1e−4; overlap of human genes correlated with miR-122 and mouse genes down-regulated by anti-miR-122; hypergeometric *P*-value=1.6e−29), without significant overlap for regulations in the opposite direction (hypergeometric single-test *P*-value>0.5). The overlap between genes negatively correlated with miR-122 in HCC and up-regulated in anti-miR-122-treated mice defines a set of putative miR-122 primary targets (Supplementary Table Ia). The overlap between genes positively correlated with miR-122 in HCC and down-regulated in anti-miR-122-treated mice defines putative secondary miR-122 targets (Supplementary Table Ib).

To further show that orthologous genes are regulated by miR-122 in the same directions in both systems, we compared their average expression levels and their relationships with miR-122 (Figure 3B). All significantly regulated transcripts on the mouse microarray that can be mapped to human orthologs were binned by the correlation of the human orthologs to miR-122 in HCC patient tissue and the average expression ratio (HCC versus non-tumor in human, antagomir treated versus

control in mouse liver) for orthologs in each bin was computed. As expected for the human transcripts, the anti-correlated genes were more highly expressed in tumor relative to non-tumor, whereas the correlated genes were more under-expressed. Similar dependence was observed in mouse liver treated by the anti-miR-122, even though the binning was based on correlation in HCC.

miR-122 regulation of mitochondrial metabolic gene network

The mechanism of repression of mitochondrially localized genes by decreasing miR-122 is not obvious. We reasoned that a direct link between the degree of induction of seed-matched genes and the magnitude of repression of mitochondrial genes through loss of miR-122 could be observed in a group of mice, as time, dose, and individual animal characteristics caused a range of responses. In fact, the mean regulations of seed-matched and mitochondrial gene sets are well correlated across the varied responses in the treated mice (Figure 4A), supporting a direct link between induction of miR-122 targets and repression of mitochondrial function.

To test whether the regulation of seed-matched genes and mitochondrial genes in human liver was directly related across the range of patient conditions, we performed a similar analysis on a separate transcriptome profiling dataset from 180 HCC, 40 cirrhotic, and 6 normal liver tissue samples. For this test, we selected genes negatively correlated with miR-122, seed matched in both mouse and human 3′UTRs, and mitochondrially localized genes positively associated with miR-122 in both mouse and human samples. Expression levels

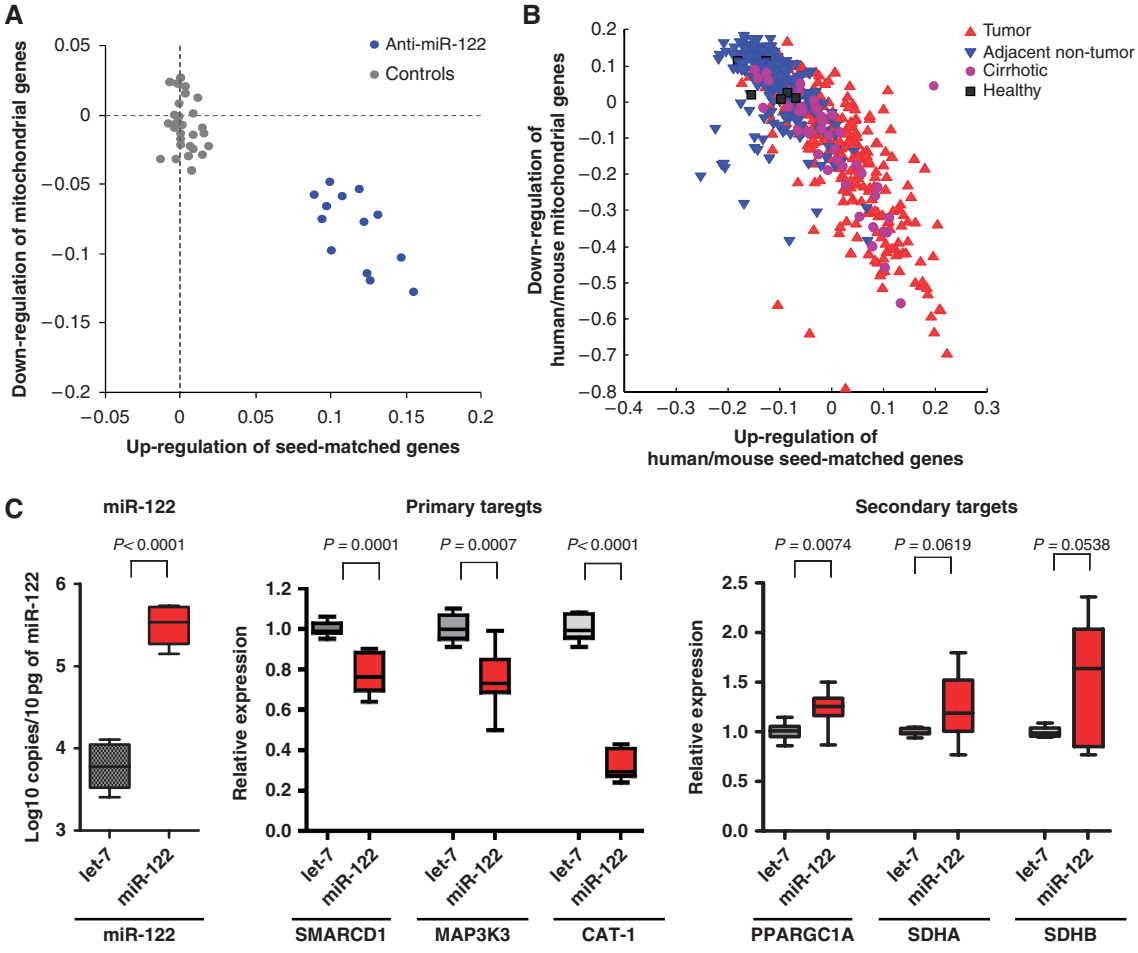

Figure 4 (**A**) Up-regulation of seed-matched genes by anti-miR-122 is correlated with down-regulation of mitochondrial genes in individual mice. Shown is the mean regulation of miR-122 seed-matched genes up-regulated by anti-miR-122 compared with the mean regulation of mitochondrially localized genes down-regulated by anti-miR-122 in individual mice treated with anti-miR-122 or control oligonucleotides for 1, 3, or 4 weeks. Correlation coefficient of mean up-regulation versus mean down-regulation within anti-miR-122-treated mice is $r=-0.66$. (**B**). Up-regulation of seed-matched genes by anti-miR-122 is correlated with down-regulation of mitochondrial genes in individual HCC patients. To confirm the relation of the seed-matched genes and the mitochondrial genes derived from the 96 HCC patients and recapitulated in the mouse liver, we included additional transcriptome profiling data from 180 HCC, 40 cirrhosis, and 6 normal liver tissues for analysis. Shown is the mean regulation, in individual HCC patients, of miR-122 seed-matched genes anti-correlated with miR-122 and up-regulated by anti-miR-122 in mouse livers, compared with the mean regulation of mitochondrially localized genes correlated with miR-122 and down-regulated in anti-miR-122-treated mouse livers. Correlation coefficient of mean regulation of the two gene sets: tumor tissue, $r=-0.73$; adjacent non-tumor tissue, $r=-0.52$; cirrhotic tissue, $r=-0.91$; healthy tissue, insufficient data points to calculate correlation. (**C**) Treatments of miR-122 mimetic altered the expression levels of seed-matched primary targets and mitochondria-related secondary targets in HCC cells. The concurrent reduced expression of primary targets SMARCD1, MAP3K3, and CAT-1, and increased expression of secondary targets PPARGC1A, SDHA, and SDHB were observed after treatment with miR-122 mimetic in PLC/PRF/5/cells.

of these gene sets were strongly anti-correlated with each other in individual HCC tumors, adjacent non-tumor tissue, and in cirrhotic livers (Figure 4B). These data suggest that the relationship observed in mouse is functionally conserved in human beings. To validate the direct correlation between miR-122 and some of the primary and secondary targets, we determined expression of two putative direct targets, SMARCD1 and MAP3K3 (MEKK3), a target described in the literature, CAT-1 (SLC7A1), and three putative secondary targets, PPARGC1A (PGC-1α), succinate dehydrogenase (SDH) subunits A and B, after transfection of miR-122 mimetic into PLC/PRF/5 HCC cells. The expressions of the seed-matched genes, SMARCD1, MAP3K3, and CAT-1 were reduced upon increased expression of miR-122, and the putative secondary target genes, PPARGC1A, SDHA, and SDHB, showed increased expression (Figure 4C). In contrast, the transfection of anti-miR-122 resulted in an increased expression of seed-matched genes and reduced expression of mitochondrial genes (Supplementary Figure 2).

Function of miR-122 in mitochondrial energy metabolism

We used functional classification of genes by total ancestry (Yu *et al*, 2007) to investigate whether common functions might link expression of miR-122 targets with mitochondrial function. We first defined a set of putative miR-122 targets: genes negatively correlated with miR-122 expression in HCC tumor and adjacent tissue with correlation coefficients <-0.4, having mouse orthologs up-regulated by anti-miR-122 with mean log10 expression ratios >0.09 and geometric mean P-values of up-regulation <0.05, as calculated by a microarray error model (Weng *et al*, 2006) over multiple animal treatments. Next, we defined a set of putative miR-122 secondary targets, applying the opposite criteria to select genes positively correlated with miR-122 in human tissue and down-regulated by anti-miR-122 in mouse. We then identified all miR-122 secondary targets connected to miR-122 targets by functional similarity (Figure 5A). The most connected secondary target, with 27 functional similarities, was PPARGC1A (PGC-1α). Functional similarity was frequently associated with more direct connections. For example, among the putative primary targets connected to PPARGC1A, MED1 (TRAP220) (Wallberg *et al*, 2003), and SMARCD1 (BAF60a) (Li *et al*, 2008) are fellow transcriptional co-activators; and LCMT1 (PPM1) (Leulliot *et al*, 2004), PPP1CC, ATF4 (CREB2), MAP3K3 (MEKK3), and MAPKAP2 (MK2) (Wu *et al*, 2001) may be involved in regulation of PPARGC1A expression. As mentioned previously, transfection of miR-122 mimetic could increase PPARGC1A expression. To further validate the link of miR-122 and PGC-1α protein, we transfected PLC/PRF/5 with miR-122-expression vector, and the increase of PGC-1α protein levels was observed (Figure 5B). Importantly, transfection of both miR-122 mimetic and miR-122-expression vector led to a significant reduction of lactate content in PLC/PRF/5 cells (Figure 5C), whereas the anti-miR-122 treatment led to an increase of lactate production in the PLC/PRF/5 cells (Supplementary Figure 3). Together, the data support the function of miR-122 in mitochondrial metabolic functions.

miR-122-regulated pathways contribute to patient survival

As anti-miR-122-treated animals tolerate the loss of miR-122 well (Jopling *et al*, 2005; Krützfeldt *et al*, 2005; Budhu *et al*, 2008; Elmén *et al*, 2008a, b), the question remained as to the relevance of loss of miR-122 function to morbidity and mortality for HCC patients. Indeed, miR-122-expression levels on their own were not significantly related to patient survival at the $P<0.05$ level (log-rank P-value=0.09 in tumor tissue and 0.17 in adjacent non-tumor tissue). However, when comparing between surviving and deceased patients, the miR-122 secondary targets were expressed at significantly higher levels in both tumor (ANOVA P-value=0.02) and adjacent non-tumor (ANOVA P-value=0.006) tissues among the survivors. Patients in the bottom 50% for expression of the miR-122 secondary targets in either tumor or adjacent non-tumor tissue showed significantly shorter survival times (Figure 6). As there is no correlation between tumor and adjacent non-tumor samples from the same patient of miR-122 levels (r=0.02) or of miR-122 secondary target levels (r=−0.06), prognostic significance of each tissue appears independent.

Discussion

Normal liver function includes building biomolecules for export to consumer tissues of the body (Yokoyama *et al*, 2005). This catabolism requires energy and liver tissue is rich in mitochondria. Loss of mitochondrial function may in turn be associated with loss of liver function. Dysregulation of normal mitochondrial functions may also contribute to cancer metabolism and hepatocarcinogenesis, as the connection between mitochondrial dysfunction and cancer is well known (Brandon *et al*, 2006). It is possible that loss of miR-122 expression in HCC may contribute to loss of liver function, a contributor to morbidity and mortality in HBV-associated HCC. We have shown that loss of expression of miR-122 positively correlated genes predicts poor survival for HCC patients. In our patient cohort, expression levels of miR-122-regulated pathways in both tumor and adjacent non-tumor tissue appear to be independently functioning as good markers of patient prognosis.

Although miR-122 negatively correlated genes were enriched for cell-cycle function in HCC (E-value=8e−18), the miR-122 seed-matched transcripts showed only random overlap with cell-cycle transcripts (single-test hypergeometric P-value=0.78). These observations suggest that there is likely no direct connection between up-regulation of potential miR-122 targets and up-regulation of the proliferative apparatus in tumor tissue. Further, we did not find strong prognostic power for patient survival in miR-122-expression levels, although a smaller study has (Coulouarn *et al*, 2009). We also did not find strong prognostic power in expression levels of proposed miR-122 direct targets, whereas expression of the putative secondary targets, transcripts positively correlated with miR-122, is predictive of patient survival. Two possible implications of these observations are that the downstream target pathways are more connected to clinical outcome than the primary targeting mechanisms and that downstream pathways may

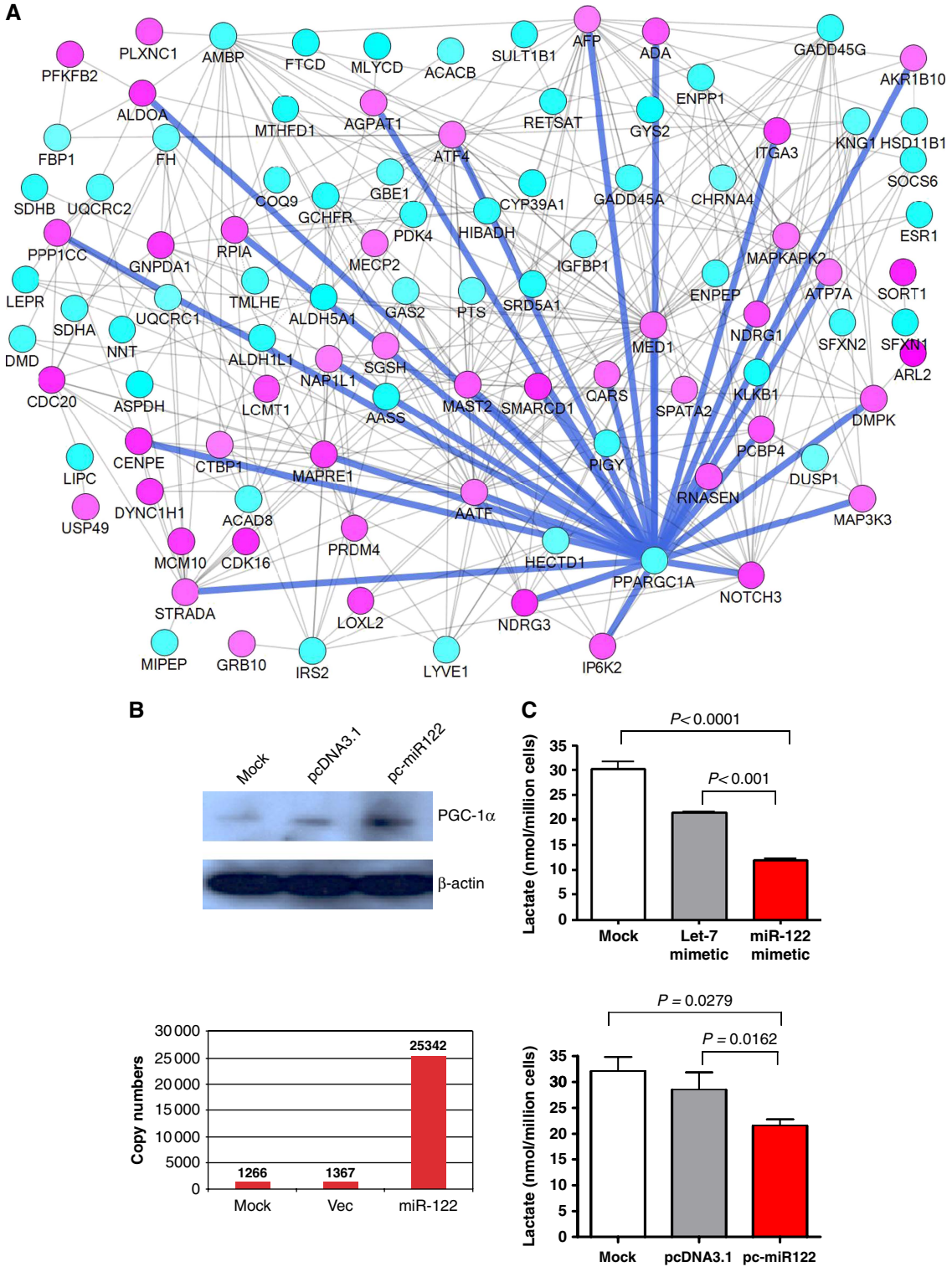

Figure 5 (**A**) Target-focused human/mouse network of miR-122-associated genes. Genes in this network were either putative miR-122 primary targets up-regulated by anti-miR-122 in mouse livers and negatively correlated with miR-122 expression in human HCC, or putative miR-122 secondary targets down-regulated by anti-miR-122 in mouse livers and positively correlated with miR-122 in human HCC. Functional similarity (Yu *et al*, 2007) connections are shown between putative primary and secondary targets. Thicker blue lines emphasize the connections to PPARGC1A, the putative secondary target with the most connections to primary targets. Color of gene ovals indicates direction of correlation with miR-122 in HKU patient samples (magenta, negative correlation; cyan, positive correlation). (**B**) Over-expression of miR-122 in HCC enhances PGC-1α protein expression. PLC/PRF/5 cells were either mock transfected, transfected with vector alone, or transfected with vector expressing miR-122. Top panel: western blot of PGC-1α protein expression in the transfected cells. Bottom panel: expression levels of miR-122 in the transfected cells, as measured by qPCR. (**C**) Altered miR-122-expression level affects lactate accumulation in PLC/PRF/5 cells. Transfection of miR-122 mimetic or miR-122-expression vector caused a decrease in lactate content in PLC/PRF/5 HCC cells. Data shown are the representative set of two independent experiments and are mean ± s.d. Source data is available for this figure at www.nature.com/msb.

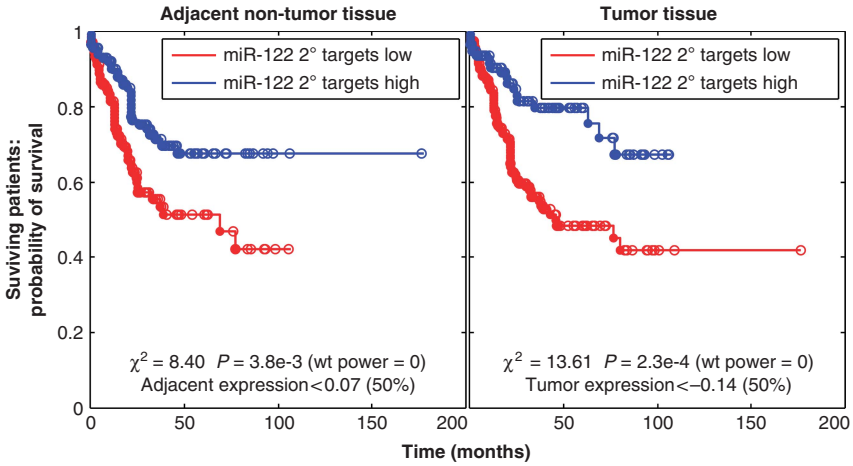

Figure 6 Expression of miR-122 secondary targets in HCC tumor and adjacent non-tumor tissue predicts patient outcome. 180 patients were classified by the mean-expression ratio in their tumors or adjacent non-tumor tissue of miR-122 secondary targets (Supplementary Table Ib). Lower expression of these genes correlates with lower expression of miR-122; however, directly measured miR-122 levels are less prognostic (P=0.092 for miR-122 in tumor tissue). Shown are Kaplan–Meier curves for survival of patients in the top versus bottom 50% of patients for miR-122 secondary target expression either in adjacent tissue (left panel) or in tumor tissue (right panel). Note that the median secondary target-expression level is 60% higher in adjacent non-tumor tissue versus tumor tissue.

form a more sensitive measure of miRNA activity than direct measurements of miRNA-expression levels (Davis *et al*, 2009).

Genes that were up- and down-regulated in HCC and in anti-miR-122-treated mice (putative primary and secondary miR-122 targets), appear to function as a biological network. A number of these genes are connected by functional similarity as determined by the total ancestry method of functional classification analysis (Yu *et al*, 2007). In addition, a number of proposed primary and secondary target genes found in this work have been previously reported to be associated in various functional networks. The networks associated with statin (an HMG-CoA reductase inhibitor to lower cholesterol levels) treatment, high-fat feeding or fasting, expression of the obesity causal gene Zfp90, and with cohesive gene expression in normal liver overlap significantly with miR-122 primary and secondary targets (Schadt *et al*, 2005, 2008; Chen *et al*, 2008).

PPARGC1A is the miR-122 secondary target most connected by functional similarity to genes up-regulated by loss of miR-122 in both human HCC and anti-miR-122-treated mice. PPARGC1A transcription is activated by cAMP-response element-binding proteins (CREB) (Wu *et al*, 2001). Among those genes connected to PPARGC1A in this study, PPP1CC negatively regulates CREB, and LCMT1 (Leulliot *et al*, 2004) activates PPP2A, which inhibits CaM-kinase activation of CREB and MEK/ERK signaling in the MAP-kinase pathway (Wu *et al*, 2001). The MAP-kinase pathway represented by MAP3K3 and MAPKAP2 among genes up-regulated by loss of miR-122 leads to phosphorylation of PPARGC1A that both activates the protein and enhances SCF/Cdc4-mediated degradation of the protein (Olson *et al*, 2008). These published observations suggest that multiple miR-122 targets may contribute to the down-regulation of PPARGC1A observed with loss of miR-122.

PPARGC1A is proposed to be the master regulator of mitochondrial biogenesis (Ventura-Clapier *et al*, 2008), suggesting that loss of PPARGC1A expression may contribute to the loss of mitochondrial gene expression correlated with loss of miR-122 expression. PPARGC1A-over-expressing mouse strains show uncontrolled mitochondrial biogenesis (Lehman *et al*, 2000), whereas PPARGC1A-knockout mouse strains show decreased expression of mitochondrial genes with strain-dependent compensatory phenotypes (Benton *et al*, 2008). PPARGC1A and HNF-4 are thought to act together to stimulate cholesterol biosynthesis (Rodgers and Puigserver, 2007), so loss of PPARGC1A may contribute to the reduction in plasma cholesterol seen in anti-miR-122-treated animals (Jopling *et al*, 2005; Esau *et al*, 2006; Elmén *et al*, 2008a, b). SMARCD1 (BAF60a), which stimulates fatty-acid oxidation in conjunction with PPARGC1A without changing its expression level (Li *et al*, 2008), is proposed to be a primary target of miR-122 in this study and in a recent publication (Gatfield *et al*, 2009), suggesting that increased fatty-acid oxidation seen with miR-122 depletion (Esau *et al*, 2006; Gatfield *et al*, 2009) may be a direct effect. Another study found that reduction of miR-122 levels in non-alcoholic steatosis was associated with increased expression of lipogenic genes (Cheung *et al*, 2008). In anti-miR-122-treated mice in this study, expression levels for genes encoding cholesterol biosynthesis and lipid metabolism are not tightly anti-correlated with expression levels of miR-122 seed-matched genes (data not shown), suggesting that the observed effects of anti-miR-122 on cholesterol and lipid synthesis may be further downstream of miR-122. Microarray studies of anti-miR-122 in high-fat-fed mice may be of interest in elucidating the connection between miR-122 and cholesterol biosynthesis.

Interestingly, down-regulation of SDH subunits A and B is associated with loss of miR-122 in both mouse and human tissues in this study. Increased expressions of both the genes were detected in cell culture after treatment with miR-122 mimetic. Loss-of-function mutations in genes encoding subunits B, C, or D of SDH lead to loss of mitochondrial function and to hereditary paraganglioma or in the case of SDHB, also to phaeochromocytoma or renal cell carcinoma (King *et al*, 2006). A decline in SDH function concomitant with the loss of miR-122 may thus increase the risk of oncogenesis.

Recently, miR-122 has been suggested to act as a tumor suppressor in HCC (Tsai *et al*, 2008; Coulouarn *et al*, 2009). In the study of Tsai *et al*, a combination of bioinformatics and tumor profiling was used to identify 45 genes as potential miR-122 targets. About half of the proposed targets were anti-correlated with miR-122 in the tumor and non-tumor tissues profiled in our study. A total of 11 of the genes were also up-regulated in the anti-miR-122-treated mouse livers we profiled, suggesting cross-species conservation of the regulations these authors identified. However, ADAM17, followed up in more depth by Tsai *et al*, was not significantly anti-correlated with miR-122 in our profiles. The study of Coulouarn *et al* found gene-expression clusters associated with high and low miR-122 levels in 32 HCC tissue samples. Genes whose increased expression was associated with lower miR-122 levels in these samples included predicted miR-122 targets and genes up-regulated in anti-miR-122-treated mice, whereas genes whose increased expression was associated with higher miR-122 levels were enriched for lipid metabolism functions and were more likely to be well expressed in control mice. This study emphasized the function of HNF1A and HNF3, transcription factors mediating hepatocyte differentiation and liver functions, in potential regulation of miR-122 expression. Our study is unable to support a primary or secondary function for these genes. HNF3 components were uncorrelated with miR-122 in tumor and non-tumor tissues profiled in our study and were not consistently regulated in anti-miR-122-treated mouse livers. HNF1A showed no significant relationship to miR-122 in tumor and non-tumor profiles; we have no data on mouse expression.

Taken together, our results imply that normal mitochondrial function in liver, including expression of mitochondrion-associated metabolic pathways, may be maintained in part by miR-122 expression. Impaired mitochondrial functions are observed in many tumor types, suggesting an alternate possibility that the observed decline in mitochondrial function in HCC may be tumor related rather than miRNA related (Jopling *et al*, 2005). Our observations that mitochondrial function pathways and miR-122 levels also decline coordinately in cirrhotic liver and in anti-miR-122-treated mouse livers argue against this explanation.

Other connections between loss of miR-122 expression and changes in liver function have been proposed. CAT-1 (SLC7A1) was shown to be a direct target of miR-122 (Chang *et al*, 2004; Jopling *et al*, 2006), and although it is negatively correlated with miR-122 levels in HCC in this study, it is unregulated in anti-miR-122-treated mouse livers profiled herein. Bcl-w, recently found to be targeted by miR-122 (Lin *et al*, 2008), was negatively correlated with miR-122 levels in HCC in this study and is up-regulated in anti-miR-122-treated mouse livers, supporting a pro-apoptotic function for miR-122 in HCC and indicating a survival advantage to its down-regulation in HCC. Expression of miR-122 precursors is known to be circadian; in a recent study, eight genes were identified as showing circadian accumulation in microarray experiments, showing up-regulation in mouse livers treated with anti-miR-122 and having 3′UTRs down-regulated by miR-122 mimetics (Gatfield *et al*, 2009). In total, 11 other genes were identified as showing up-regulation by anti-miR-122 and having 3′UTRs down-regulated by miR-122 mimetics, but without circadian accumulation. In this study, 13 of these 19 genes were up-regulated by anti-miR-122 treatment in mice, including 7 of the 8 genes showing circadian accumulation. However, only one gene, SMARCD1 (BAF60a), also showed expression negatively correlated with miR-122 expression in our HCC samples, emphasizing the importance of cross-species analysis. Cyclin G1, found by others (Gramantieri *et al*, 2007) to be anti-correlated with miR-122 in HCC, was not significantly correlated or anti-correlated with miR-122 in our samples. Similarly, although N-myc has been suggested as a target of miR-122 (Girard *et al*, 2008), its expression levels are not significantly correlated or anti-correlated to miR-122 levels in this study.

Other published studies indicate that miR-122 is a host factor for HCV replication (Jopling *et al*, 2005, 2006; Shan *et al*, 2007; Chang *et al*, 2008; Henke *et al*, 2008; Lupberger *et al*, 2008) and show that HCV-infected HCC patients usually do not show a reduction in and may in fact show an increase in miR-122 expression (Varnholt *et al*, 2008), although higher miR-122 levels have also been shown to predict better response of HCV patients to standard therapy (Sheikh *et al*, 2008). HCV appears to target mitochondria directly causing liver dysfunction (Sarasin-Filipowicz *et al*, 2009) by a route not dependent on decreasing miR-122 expression.

The primary targets of an miRNA may be distributed over a variety of functional categories while resulting in a coordinated secondary response, potentially through synergistic action (Linsley *et al*, 2007). In our study, we found increased lactate production in tissue culture cells after treatment with anti-miR-122. Reduced mitochondrial oxidative phosphorylation is commonly observed in cancer cells, and we postulate that the reduced expression of miR-122 may contribute to this effect in HCC. In light of the observed connection between miR-122 expression and mitochondrial function pathways in liver, we speculate that increasing miR-122 expression may possibly improve mitochondrial function in liver and perhaps in liver tumor tissues. Therefore, it is of great interest to determine the phenotypic changes of HCC after miR-122 targeting delivery in our established HCC mouse models (Zender *et al*, 2008; Liu *et al*, 2009).

Our findings reveal potential new biological functions of miR-122 in liver physiology. We have observed the decrease of miR-122, a liver-specific miRNA, in HBV-associated HCC, and loss of miR-122 appears to correlate with the decrease of mitochondrion-related metabolic pathway gene expression in HCC and in non-tumor liver tissues, a result that is consistent with the outcome of treatment of mice with anti-miR-122 and is of prognostic significance for HCC patients. Further investigation will be conducted to dissect the regulatory function of miR-122 on mitochondrial metabolism in HCC.

Materials and methods

Tissue samples

For human HCC patient samples, resected tumor and adjacent non-tumor liver tissues were collected from patients who had undergone hepatectomy for curative treatment of HCC at Queen Mary Hospital, Pokfulam, Hong Kong between 1990 and 2007. Informed consents were obtained from patients regarding the use of the liver specimens for research. Demographic and clinicopathologic features are summarized in Supplementary Table II and elsewhere (Yi *et al*, 2008; Hao *et al*, 2009; Lee *et al*, 2009; Xu *et al*, 2009).

Animal care and treatments

All animal experiments were conducted according to the Institutional American Association for the Accreditation of Laboratory Animal Care Guidelines. Male C57BL/6 mice were obtained from The Jackson Laboratory and were housed four to five animals per cage with a 12-h light/dark cycle. Oligonucleotides were dissolved in saline and administered to mice based on body weight by intraperitoneal injection. In one treatment regimen, animals were given four doses of 100 mg ASO/kg body weight, administered every other day, and killed 1 day after the last dose. Animals treated for 4 weeks were treated twice weekly with 50 mg ASO/kg body weight, and killed 2 days after the last dose. Mice were killed in the morning, and liver was removed for further analysis. There were no statistically significant elevations in plasma transaminase levels after either treatment regimen and no significant histological findings.

Reagents

Nucleic-acid reagents used in this study were as follows. The miR-122 mimetic consisted of a 5′-UGGAGUGUGACAAUGGUGUUUG-3′ guide strand annealed to a [iB]AACACCAUUGUCACACUCGAAU[iB] passenger strand, where iB represents an inverted abasic cap. The Let-7 mimetic consisted of a 5′-UGAGGUAGUAGGUUGUAUAGUU-3′guide strand annealed to a [iB]CUAUACAACCUACUACCUGAAU[iB] passenger strand. For *in vitro* experiments, the anti-miR-122 antagomir consisted of a single strand, 5′-dCs;dCs;lnaAs;dTs;dTs;lnaGs;dTs; dCs;lnaAs;dCs;dAs;lna-5methylCs;dTs;dCs;lna-5methylCs;dAs-3′. The control antagomir consisted of a single strand, 5′-lna-5methylCs; dCs;lnaAs;dTs;dTs;lna-5methylCs;lnaTs;dCs;dAs;lna-5methylCs;dAs; lna-5methylCs;dTs;lnaGs;lna-5methylCs-3′. For *in vivo* experiments, antagomirs were 2′-O-methoxyethyl (2′-MOE) phosphorothioate modified. The anti-miR-122 antagomir consisted of a single strand, 5′-ACAAACACCATTGTCACACTCCA-3′. The control antagomir consisted of a single strand, 5′-CCTTCCCTGAAGGTTCCTCCTT-3′.

RNA analysis

Total RNA was purified from mouse *in vivo* samples using an RNeasy kit (Qiagen, Valencia, CA). RNA from anti-miR-122-treated mice was compared with RNA from mice injected with phosphate-buffered saline. Three to five mice were analyzed for each treatment or control group. Microarray hybridizations were performed as described (Jackson *et al*, 2003). Isolation of RNA from human samples was achieved using the following procedures. The milled tissue samples were homogenized in cryopreservation tubes with a vortex mixer after addition of 750–1000 μl of TRIzol reagent. Chloroform was added to the TRIzol/GITC lysate (1:5) to facilitate separation of the organic and aqueous components using the phaselock (Eppendorf) system. The aqueous supernatant was further purified using the Promega SV-96 total RNA kit, incorporating a DNase treatment during the procedure. Isolated total RNA samples were then assayed for quality (Agilent Bioanalyzer) and yield (Ribogreen) metrics. Hybridization, labeling, and scanning of microarrays were completed following the manufacturer's recommendations (Affymetrix). Human samples were profiled on a custom Affymetrix array, RM-HU01Aa520485 RSTA Custom Affymetrix 1.0. Mouse samples were profiled on a custom Agilent array, RSTA Mouse 3.0 A1. The miRNA profiling was performed by custom quantitative PCR assays as described (Raymond *et al*, 2005). Microarray data transformation and analysis was performed as described (Irizarry *et al*, 2003; Jackson *et al*, 2003; Eklund *et al*, 2006). Upon publication of this manuscript, microarray data will be available in GEO (http://www.ncbi.nlm.nih.gov/geo/info/linking.html), under accession number GSE22058 (released on 4 June 2010).

Analysis methods

Regulated transcripts were identified in microarray gene-expression signatures using a *P*-value cut-off ($P<0.01$ or $P<0.05$, as specified). No cuts were placed on fold change in expression unless specified. Data were analyzed using Rosetta Resolver™ and MATLAB™ software. Regulated transcripts were tested for enrichment of transcripts belonging to gene sets in the GO Cellular Component (Ashburner *et al*, 2000) and KEGG Pathways (Kanehisa *et al*, 2008) annotation sources or of transcripts containing one or more copies of a hexamer sequence in the 3′UTR relative to a background set (i.e. the set of genes represented on the microarray) using the hypergeometric distribution. The *P*-value for enrichment of each gene set in an annotation source or of each of 4096 possible hexamers was subjected to Bonferroni's correction.

Tissue culture

PLC/PRF/5 and MHCC-97L cells were transfected with 10 nM of either let-7 or miR-122 mimetic, and cell lysates were collected 48 h post-transfection using TRIzol (Invitrogen, Carlsbad, CA). For the miR-122-knockdown assay, PLC/PRF/5 cells were transfected with 80 mM of either miR-122 antisense or control miR-122 antisense, and cell lysates were collected 48 h post-transfection using TRIzol (Invitrogen). Real-time qPCR assays were performed to evaluate the expression levels of CAT-1, SMARCD1, MAP3K3, PPARGC1A, SHDA, and SDHB using Power SYBR Green PCR Master Mix (Applied Biosystems, Foster City, CA). For detection of miR-122 expression, TaqMan MicroRNA Assay specific for miR-122 (Applied Biosystems) was used, and procedures were in accordance with manufacturer's protocol. The numbers of miR-122 copies in samples were quantified with a standard curve.

The miR-122-expression vector was generated by cloning of the genomic region containing mature miR-122 sequence and its 5′- and 3′-flanking sequence into pcDNA3.1 vector (Invitrogen). PLC/PRF/5 cells were transfected with 2 μg per well of purified miR-122 plasmids in six-well plates using Lipofectamine 2000 (Invitrogen) as previously described (Liu *et al*, 2010). For western blot analysis, cell lysates were prepared in RIPA buffer 48 h post-transfection and probed with a rabbit monoclonal antibody (clone 3G6) against PGC-1α (1:1000 dilution; Cell Signaling Inc., Beverly, MA), and the blot was developed using chemiluminescent detection substrate solution (Millipore, Billerica, MA).

Lactate assay

Cellular lactate level of PLC/PRF/5 cells after miR-122 antagomir treatment or ectopic expression of miR-122 was determined using a commercial lactate assay kit (BioVision, Mountain View, CA) as described by Christofk *et al* (2008). All procedures were in accordance with the manufacturer's instruction.

Supplementary information

Supplementary information is available at the *Molecular Systems Biology* website (http://www.nature.com/msb).

Acknowledgements

The work is partly supported by the small project fund of the Hong Kong University, NMRC Block Vote, and Start-up fund of the National University of Singapore to JML. We gratefully acknowledge Sheung-Tat Fan of Queen Mary Hospital for his expert clinical advice in HCC, Douglas Bassett and Alan Sachs of Merck and Co., Inc. for guidance and support of these studies, and C Frank Bennett and Christy Esau of Isis Pharmaceuticals, Inc. for provision of the anti-miR-122-treated mouse liver samples and for helpful discussions. In addition, we thank Ke Hao, Tao Xie, Steven Bartz, Walter Strapps, Lyndon Mitnaul, Luiz Miguel Camargo, Robert Phillips, Peter Shaw, Eric Schadt, Peter Linsley, and Carolyn Buser-Dopner of Merck and Co., Inc. for scientific input and helpful discussions.

Conflict of interest

The authors declare that they have no conflict of interest.

References

Ashburner M, Ball CA, Blake JA, Botstein D, Butler H, Cherry JM, Davis AP, Dolinski K, Dwight SS, Eppig JT, Harris MA, Hill DP, Issel-Tarver L, Kasarskis A, Lewis S, Matese JC, Richardson JE, Ringwald M, Rubin GM, Sherlock G (2000) Gene ontology: tool for the unification of biology. The Gene Ontology Consortium. *Nat Genet* **25:** 25–29

Benton CR, Wright DC, Bonen A (2008) PGC-1alpha-mediated regulation of gene expression and metabolism: implications for nutrition and exercise prescriptions. *Appl Physiol Nutr Metab* **33:** 843–862

Brandon M, Baldi P, Wallace DC (2006) Mitochondrial mutations in cancer. *Oncogene* **25:** 4647–4662

Budhu A, Jia HL, Forgues M, Liu CG, Goldstein D, Lam A, Zanetti KA, Ye QH, Qin LX, Croce CM, Tang ZY, Wang XW (2008) Identification of metastasis-related microRNAs in hepatocellular carcinoma. *Hepatology* **47:** 897–907

But DY, Lai CL, Yuen MF (2008) Natural history of hepatitis-related hepatocellular carcinoma. *World J Gastroenterol* **14:** 1652–1656

Chang J, Guo JT, Jiang D, Guo H, Taylor JM, Block TM (2008) Liver-specific microRNA miR-122 enhances the replication of hepatitis C virus in nonhepatic cells. *J Virol* **82:** 8215–8223

Chang J, Nicolas E, Marks D, Sander C, Lerro A, Buendia MA, Xu C, Mason WS, Moloshok T, Bort R, Zaret KS, Taylor JM (2004) miR-122, a mammalian liver-specific microRNA, is processed from hcr mRNA and may downregulate the high affinity cationic amino acid transporter CAT-1. *RNA Biol* **1:** 106–113

Chen Y, Zhu J, Lum PY, Yang X, Pinto S, MacNeil DJ, Zhang C, Lamb J, Edwards S, Sieberts SK, Leonardson A, Castellini LW, Wang S, Champy MF, Zhang B, Emilsson V, Doss S, Ghazalpour A, Horvath S, Drake TA *et al* (2008) Variations in DNA elucidate molecular networks that cause disease. *Nature* **452:** 429–435

Cheung O, Puri P, Eicken C, Contos MJ, Mirshahi F, Maher JW, Kellum JM, Min H, Luketic VA, Sanyal AJ (2008) Nonalcoholic steatohepatitis is associated with altered hepatic MicroRNA expression. *Hepatology* **48:** 1810–1820

Christofk HR, Vander Heiden MG, Harris MH, Ramanathan A, Gerszten RE, Wei R, Fleming MD, Schreiber SL, Cantley LC (2008) The M2 splice isoform of pyruvate kinase is important for cancer metabolism and tumour growth. *Nature* **452:** 230–233

Coulouarn C, Factor VM, Andersen JB, Durkin ME, Thorgeirsson SS (2009) Loss of miR-122 expression in liver cancer correlates with suppression of the hepatic phenotype and gain of metastatic properties. *Oncogene* **28:** 3526–3536

Croce CM (2008) Oncogenes and cancer. *N Engl J Med* **358:** 502–511

Davis S, Propp S, Freier SM, Jones LE, Serra MJ, Kingerger G, Bhat B, Swayze EE, Bennett CF, Esau C (2009) Potent inhibition of microRNA *in vivo* without degradation. *NAR* **37:** 70–77

Eklund AC, Turner LR, Chen P, Jensen RV, deFeo G, Kopf-Sill AR, Szallasi Z (2006) Replacing cRNA targets with cDNA reduces microarray cross-hybridization. *Nat Biotechnol* **24:** 1071–1073

Elmén J, Lindow M, Schütz S, Lawrence M, Petri A, Obad S, Lindholm M, Hedtjärn M, Hansen HF, Berger U, Gullans S, Kearney P, Sarnow P, Straarup EM, Kauppinen S (2008a) LNA-mediated microRNA silencing in non-human primates. *Nature* **452:** 896–899

Elmén J, Lindow M, Silahtaroglu A, Bak M, Christensen M, Lind-Thomsen A, Hedtjärn M, Hansen JB, Hansen HF, Straarup EM, McCullagh K, Kearney P, Kauppinen S (2008b) Antagonism of microRNA-122 in mice by systemically administered LNA-antimiR leads to up-regulation of a large set of predicted target mRNAs in the liver. *Nucleic Acids Res* **36:** 1153–1162

Esau C, Davis S, Murray SF, Yu XX, Pandey SK, Pear M, Watts L, Booten SL, Graham M, McKay R, Subramaniam A, Propp S, Lollo BA, Freier S, Bennett CF, Bhanot S, Monia BP (2006) miR-122 regulation of lipid metabolism revealed by *in vivo* antisense targeting. *Cell Metab* **3:** 87–98

Gatfield D, Le Martelot G, Vejnar CE, Gerlach D, Schaad O, Fleury-Olela F, Ruskeepää AL, Oresic M, Esau CC, Zdobnov EM, Schibler U (2009) Integration of microRNA miR-122 in hepatic circadian gene expression. *Genes Dev* **23:** 1313–1326

Girard M, Jacquemin E, Munnich A, Lyonnet S, Henrion-Caude A (2008) miR-122, a paradigm for the role of microRNAs in the liver. *J Hepatol* **48:** 648–656

Gramantieri L, Ferracin M, Fornari F, Veronese A, Sabbioni S, Liu CG, Calin GA, Giovannini C, Ferrazzi E, Grazi GL, Croce CM, Bolondi L, Negrini M (2007) Cyclin G1 is a target of miR-122a, a microRNA frequently down-regulated in human hepatocellular carcinoma. *Cancer Res* **67:** 6092–6099

Hao K, Luk JM, Lee NPY, Mao M, Zhang C, Ferguson MD, Lamb J, Dai H, Ng IO, Sham PC, Poon RTP (2009) Predicting prognostics in hepatocellular carcinoma after curative surgery with common clinicopathological parameters. *BMC Cancer* **9:** 389

Henke JI, Goergen D, Zheng J, Song Y, Schüttler CG, Fehr C, Jünemann C, Niepmann M (2008) microRNA-122 stimulates translation of hepatitis C virus RNA. *EMBO J* **27:** 3300–3310

Irizarry RA, Bolstad BM, Collin F, Cope LM, Hobbs B, Speed TP (2003) Summaries of Affymetrix GeneChip probe level data. *Nucleic Acids Res* **31:** e15

Jackson AL, Bartz SR, Schelter J, Kobayashi SV, Burchard J, Mao M, Li B, Cavet G, Linsley PS (2003) Expression profiling reveals off-target gene regulation by RNAi. *Nat Biotechnol* **21:** 635–637

Jopling CL, Norman KL, Sarnow P (2006) Positive and negative modulation of viral and cellular mRNAs by liver-specific microRNA miR-122. *Cold Spring Harb Symp Quant Biol* **71:** 369–376

Jopling CL, Yi M, Lancaster AM, Lemon SM, Sarnow P (2005) Modulation of hepatitis C virus RNA abundance by a liver-specific MicroRNA. *Science* **309:** 1577–1581

Kanehisa M, Araki M, Goto S, Hattori M, Hirakawa M, Itoh M, Katayama T, Kawashima S, Okuda S, Tokimatsu T, Yamanishi Y (2008) KEGG for linking genomes to life and the environment. *Nucleic Acids Res* **36:** D480–D484

King A, Selak MA, Gottlieb E (2006) Succinate dehydrogenase and fumarate hydratase: linking mitochondrial dysfunction and cancer. *Oncogene* **25:** 4675–4682

Krützfeldt J, Rajewsky N, Braich R, Rajeev KG, Tuschl T, Manoharan M, Stoffel M (2005) Silencing of microRNAs *in vivo* with 'antagomirs'. *Nature* **438:** 685–689

Kutay H, Bai S, Datta J, Motiwala T, Pogribny I, Frankel W, Jacob ST, Ghoshal K (2006) Downregulation of miR-122 in the rodent and human hepatocellular carcinomas. *J Cell Biochem* **99:** 671–678

Lagos-Quintana M, Rauhut R, Yalcin A, Meyer J, Lendeckel W, Tuschl T (2002) Identification of tissue-specific microRNAs from mouse. *Curr Biol* **12:** 735–739

Lee NP, Chen L, Lin MC, Tsang FH, Yeung C, Poon RT, Peng J, Leng X, Beretta L, Sun S, Day PJ, Luk JM (2009) Proteomic expression signature distinguishes cancerous and nonmalignant tissues in hepatocellular carcinoma. *J Proteome Res* **8:** 1293–1303

Lee NP, Cheung ST, Poon RT, Fan ST, Luk JM (2007) Genomic and proteomic biomarkers for diagnosis and prognosis of hepatocellular carcinoma. *Biomarkers Med* **1:** 273–284

Lehman JJ, Barger PM, Kovacs A, Saffitz JE, Medeiros DM, Kelly DP (2000) Peroxisome proliferator-activated receptor gamma coactivator-1 promotes cardiac mitochondrial biogenesis. *J Clin Invest* **106:** 847–856

Leulliot N, Quevillon-Cheruel S, Sorel I, de La Sierra-Gallay IL, Collinet B, Graille M, Blondeau K, Bettache N, Poupon A, Janin J, van Tilbeurgh H (2004) Structure of protein phosphatase methyltransferase 1 (PPM1), a leucine carboxyl methyltransferase involved in the regulation of protein phosphatase 2A activity. *J Biol Chem* **279:** 8351–8358

Li S, Liu C, Li N, Hao T, Han T, Hill DE, Vidal M, Lin JD (2008) Genome-wide coactivation analysis of PGC-1alpha identifies BAF60a as a regulator of hepatic lipid metabolism. *Cell Metab* **8:** 105–117

Lim LP, Lau NC, Garrett-Engele P, Grimson A, Schelter JM, Castle J, Bartel DP, Linsley PS, Johnson JM (2005) Microarray analysis shows that some microRNAs downregulate large numbers of target mRNAs. *Nature* **433:** 769–773

Lin CJ, Gong HY, Tseng HC, Wang WL, Wu JL (2008) miR-122 targets an anti-apoptotic gene, Bcl-w, in human hepatocellular carcinoma cell lines. *Biochem Biophys Res Commun* **357:** 315–320

Linsley PS, Schelter J, Burchard J, Kibukawa M, Martin MM, Bartz SR, Johnson JM, Cummins JM, Raymond CK, Dai H, Chau N, Cleary M, Jackson AL, Carleton M, Lim L (2007) Transcripts targeted by the microRNA-16 family cooperatively regulate cell cycle progression. *Mol Cell Biol* **27:** 2240–2252

Liu AM, Poon RT, Luk JM (2010) MicroRNA-375 targets Hippo-signaling effector YAP in liver cancer and inhibits tumor properties. *Biochem Biophys Res Commun* **394:** 623–627

Liu LX, Lee NP, Chan VW, Xue W, Zender L, Zhan Y, Mao M, Dai H, Wang XL, Xu MZ, Lee TK, Ng IO, Chen Y, Kung H, Lowe SW, Poon RT, Wang JH, Luk JM (2009) Targeting cadherin-17 inactivates Wnt signaling and inhibits tumor growth in liver carcinoma. *Hepatology* **50:** 1453–1463

Lupberger J, Brino L, Baumert TF (2008) RNAi: a powerful tool to unravel hepatitis C virus-host interactions within the infectious life cycle. *J Hepatol* **48:** 523–525

Olson BL, Hock MB, Ekholm-Reed S, Wohlschlegel JA, Dev KK, Kralli A, Reed SI (2008) SCFCdc4 acts antagonistically to the PGC-1alpha transcriptional coactivator by targeting it for ubiquitin-mediated proteolysis. *Genes Dev* **22:** 252–264

Parkin DM, Bray F, Ferlay J, Pisani P (2005) Global cancer statistics, 2002. *CA Cancer J Clin* **55:** 74–108

Poon RT, Ng IO, Fan ST, Lai EC, Lo CM, Liu CL, Wong J (2001) Clinicopathologic features of long-term survivors and disease-free survivors after resection of hepatocellular carcinoma: a study of a prospective cohort. *J Clin Oncol* **19:** 3037–3044

Raymond CK, Roberts BS, Garrett-Engele P, Lim LP, Johnson JM (2005) Simple, quantitative primer-extension PCR assay for direct monitoring of microRNAs and short-interfering RNAs. *RNA* **11:** 1737–1744

Rodgers JT, Puigserver P (2007) Fasting-dependent glucose and lipid metabolic response through hepatic sirtuin 1. *Proc Natl Acad Sci USA* **104:** 12861–12866

Sarasin-Filipowicz M, Krol J, Markiewicz I, Heim MH, Filipowicz W (2009) Decreased levels of microRNA miR-122 in individuals with hepatitis C responding poorly to interferon therapy. *Nat Med* **15:** 31–33

Schadt EE, Lamb J, Yang X, Zhu J, Edwards S, Guhathakurta D, Sieberts SK, Monks S, Reitman M, Zhang C, Lum PY, Leonardson A, Thieringer R, Metzger JM, Yang L, Castle J, Zhu H, Kash SF, Drake TA, Sachs A *et al* (2005) An integrative genomics approach to infer causal associations between gene expression and disease. *Nat Genet* **37:** 710–717

Schadt EE, Molony C, Chudin E, Hao K, Yang X, Lum PY, Kasarskis A, Zhang B, Wang S, Suver C, Zhu J, Millstein J, Sieberts S, Lamb J, Guhathakurta D, Derry J, Storey JD, Avila-Campillo I, Kruger MJ, Johnson JM *et al* (2008) Mapping the genetic architecture of gene expression in human liver. *PLoS Biol* **6:** e107

Shan Y, Zheng J, Lambrecht RW, Bonkovsky HL (2007) Reciprocal effects of micro-RNA-122 on expression of heme oxygenase-1 and hepatitis C virus genes in human hepatocytes. *Gastroenterology* **133:** 1166–1174

Sheikh MY, Choi J, Qadri I, Friedman JE, Sanyal AJ (2008) Hepatitis C virus infection: molecular pathways to metabolic syndrome. *Hepatology* **47:** 2127–2133

Sun S, Lee NP, Poon RT, Fan ST, He QY, Lau GK, Luk JM (2007) Oncoproteomics of hepatocellular carcinoma: from cancer markers' discovery to functional pathways. *Liver Int* **27:** 1021–1038

Tsai W, Hsu P, Lai T, Chau G, Lin C, Chen C, Lin C, Liao Y, Wang J, Chau Y, Hsu M, Hsiao M, Huang H, Tsou A (2008) MicroRNA-122, a tumor suppressor microRNA that regulates intrahepatic metastasis of hepatocellular carcinoma. *Hepatology* **49:** 1571–1582

Varnholt H, Drebber U, Schulze F, Wedemeyer I, Schirmacher P, Dienes HP, Odenthal M (2008) MicroRNA gene expression profile of hepatitis C virus-associated hepatocellular carcinoma. *Hepatology* **47:** 1223–1232

Ventura-Clapier R, Garnier A, Veksler V (2008) Transcriptional control of mitochondrial biogenesis: the central role of PGC-1alpha. *Cardiovasc Res* **79:** 208–217

Wallberg AE, Yamamura S, Malik S, Spiegelman BM, Roeder RG (2003) Coordination of p300-mediated chromatin remodeling and TRAP/mediator function through coactivator PGC-1alpha. *Mol Cell* **12:** 1137–1149

Weng L, Dai H, Zhan Y, He Y, Stepaniants SB, Bassett DE (2006) Rosetta error model for gene expression analysis. *Bioinformatics* **22:** 1111–1121

Wu GY, Deisseroth K, Tsien RW (2001) Activity-dependent CREB phosphorylation: convergence of a fast, sensitive calmodulin kinase pathway and a slow, less sensitive mitogen-activated protein kinase pathway. *Proc Natl Acad Sci USA* **98:** 2808–2813

Xu MZ, Yao TJ, Lee NP, Ng IO, Chan YT, Zender L, Lowe SW, Poon RT, Luk JM (2009) Yes-associated protein is an independent prognostic marker in hepatocellular carcinoma. *Cancer* **115:** 4576–4585

Yi X, Luk JM, Lee NP, Peng J, Leng X, Guan XY, Lau GK, Beretta L, Fan ST (2008) Association of mortalin (HSPA9) with liver cancer metastasis and prediction for early tumor recurrence. *Mol Cell Proteomics* **7:** 315–325

Yokoyama T, Banta S, Berthiaume F, Nagrath D, Tompkins RG, Yarmush ML (2005) Evolution of intrahepatic carbon, nitrogen, and energy metabolism in a D-galactosamine-induced rat liver failure model. *Metab Eng* **7:** 88–103

Yu H, Jansen R, Stolovitzky G, Gerstein M (2007) Total ancestry measure: quantifying the similarity in tree-like classification, with genomic applications. *Bioinformatics* **23:** 2163–2173

Zender L, Xue W, Zuber J, Semighini CP, Krasnitz A, Ma B, Zender P, Kubicka S, Luk JM, Schirmacher P, McCombie WR, Wigler M, Hicks J, Hannon GJ, Powers S, Lowe SW (2008) An oncogenomics-based *in vivo* RNAi screen identifies tumor suppressors in liver cancer. *Cell* **135:** 852–864